Check for updates

Geophysical Research Letters

RESEARCH LETTER
10.1029/2023GL103861

Asymmetric Impacts of El Niño Development and Decay Stages on the Hadley Circulation

Juan Feng[1], Xuanliang Ji[1,2], Jianping Li[3,4], and Enye He[2]

[1]State Key Laboratory of Remote Sensing Science, Faculty of Geographical Science, Beijing Normal University, Beijing, China, [2]Key Laboratory of Research on Marine Hazards Forecasting, National Marine Environmental Forecasting Center, Ministry of Natural Resources, Beijing, China, [3]Frontiers Science Center for Deep Ocean Multi-spheres and Earth System/ Key Laboratory of Physical Oceanography/Academy of the Future Ocean, Ocean University of China, Qingdao, China, [4]Laoshan Laboratory, Qingdao, China

Key Points:

- The discrepancy in previous studies regarding the impacts of El Niño on the HC is caused by the stage shift of El Niño
- El Niño development and decay stages have distinct impacts on HC anomalies due to their associated spatial distribution of SST anomalies
- Theoretical results imply that shifts in SST meridional gradients are a key factor deciding where anomalous meridional circulation occurs

Supporting Information:

Supporting Information may be found in the online version of this article.

Correspondence to:

X. Ji,
jixl@nmefc.cn

Citation:

Feng, J., Ji, X., Li, J., & He, E. (2023). Asymmetric impacts of El Niño development and decay stages on the Hadley circulation. *Geophysical Research Letters*, *50*, e2023GL103861. https://doi.org/10.1029/2023GL103861

Received 28 MAR 2023
Accepted 30 MAY 2023

© 2023. The Authors.
This is an open access article under the terms of the Creative Commons Attribution License, which permits use, distribution and reproduction in any medium, provided the original work is properly cited.

Abstract The impact of El Niño on the Hadley Circulation (HC) has been a topic of previous studies, but the results have been inconclusive. We study how El Niño affects the HC during different stages of its cycle. In development years, the HC anomaly shows an equatorial quasi-symmetric pattern, while in decay years, it shows an asymmetric pattern. This resolves previous discrepancies among studies about El Niño's impacts on the HC. The differences in tropical sea surface temperature (SST) during different stages of El Niño cause differences in SST meridional gradients, which determine the location of convergence. This explains why the HC anomalies have different spatial structures during El Niño development and decay years. Our results show that the meridional distribution of SST during different El Niño stages has significantly distinct impacts on meridional circulation and clarify the differences in El Niño's effects on climate.

Plain Language Summary El Niño is a powerful source of year-to-year climate variability, with significant impacts on the Hadley Circulation (HC), one of the most important large-scale atmospheric circulations affecting precipitation and drought in the tropics and subtropics. It has been reported that the spatial distribution and magnitude of sea surface temperature (SST) anomalies under El Niño events can influence the long-term variability of HC. However, the impact is still inconclusive. Detailed research on how El Niño events modulate the HC is necessary. We investigate the impacts of the meridional gradient of anomalous SST during El Niño development and decay stages on the spatial structure of the HC. The results indicate that the distinct effects of different stages on the HC are mainly due to their associated SST meridional structures. The results explain why the deduced influences of El Niño on the HC in previous work were different. When considering the impacts of El Niño, the stage of the event must be considered. Furthermore, the physical mechanisms that significantly affect the HC in different stages are explained through theory and data analysis. These results and mechanisms help further our understanding of the climate impacts of El Niño and the variability of the HC.

1. Introduction

The El Niño-Southern Oscillation (ENSO) is the most prominent interannual climate variability mode and is characterized by fluctuations in the sea surface temperature (SST) and atmospheric pressure in the Pacific Ocean (Bjerknes, 1969; Timmermann et al., 2018). Researches have highlighted that there are substantial differences in SST meridional structure across different regions during the El Niño event (Feng et al., 2019; McGregor et al., 2012; Yu et al., 2022). During the development and decay stages of El Niño, SST anomalies occur globally. El Niño is accompanied by positive SST anomalies in the equatorial central-eastern Pacific Ocean, which can shift tropical convections and excite the Indian Ocean dipole mode, as well as SST fluctuations in the tropical Atlantic (Ham et al., 2021; McCreary et al., 2005). As El Niño decays, it triggers atmospheric teleconnections that lead to significantly positive SST anomalies in the northern tropical Atlantic and Indian Oceans (Jiang & Li, 2019; Schott et al., 2009). Additionally, during the decay of El Niño, the westerly winds on the sides of the equatorial tropical Pacific weaken and decay unevenly, causing SST to display different anomalous signs on the flanks of the equator over the tropical Pacific (Song et al., 2022; Stuecker et al., 2015). Consequently, large differences in the associated SST anomalies are observed during different phases of ENSO.

The Hadley Circulation (HC) is a significant component of the mean meridional circulation (Hadley, 1735) that strongly regulates climate systems. The interannual variability of the HC is classified into two dominant modes:

19448007, 2023, 11, Downloaded from https://agupubs.onlinelibrary.wiley.com/doi/10.1029/2023GL103861 by Ocean University Of China, Wiley Online Library on [07/06/2023]. See the Terms and Conditions (https://onlinelibrary.wiley.com/terms-and-conditions) on Wiley Online Library for rules of use; OA articles are governed by the applicable Creative Commons License

an equatorial asymmetric mode and an equatorial quasi-symmetric mode. Previous studies have interpreted that the equatorial quasi-symmetric mode of the HC is connected to El Niño (e.g., Feng & Li, 2013; Ma & Li, 2008; Oort & Yienger, 1996). Meanwhile, it has been illustrated that the occurrence of El Niño events could contribute to the asymmetric mode of the HC (e.g., Feng et al., 2019; Guo & Tan, 2018a; Zhang & Wang, 2013). The equatorial asymmetric and quasi-symmetric modes are linearly independent; however, both are related to the ENSO. This indicates that the influences of El Niño on the HC are still inconclusive.

On the other hand, studies have demonstrated that the spatial distribution of the HC is sensitive about underlying thermal structures (e.g., Hu et al., 2018; Nguyen et al., 2013; Seager et al., 2003; Zaplotnik et al., 2022). The anomalous distribution of the meridional circulation is notably influenced by the location and distribution of the heating profile, including its deviation from the equator or its position along the equator (e.g., Bordoni & Schneider, 2010; Fang & Tung, 1999; Numaguti, 1995). When an El Niño event develops or decays, it is associated with SST anomalies across the tropical oceans (Ham et al., 2021; McCreary et al., 2005; Stuecker et al., 2015). Such anomalous SSTs can alter the spatial structure of SST, which further impacts HC variability by modulating air–sea boundary layer dynamics and atmospheric thermal structure (Freitas et al., 2016; Oort & Yienger, 1996). Studies by Feng et al. (2016) and Hoskins et al. (2020) indicate that nonuniform (uniform) variations of SST can result in a varied meridional gradient of SST, potentially influencing the spatial distribution of the HC.

These findings suggest that the variation in the HC is dependent on underlying thermal structures, which are subject to variation along with the occurrence of El Niño. Previous research has emphasized the significant impact of El Niño on tropical SST in different phases. However, the anomalous characteristics of SST in different phases and its impact on the HC remain unclear. Moreover, previous studies on the relationship between El Niño and the HC have mainly been performed from the perspective of HC variability, and less attention has been given to the impact of different stages of El Niño events on the HC. Therefore, the present work aims to investigate the influences of El Niño on the HC from the El Niño cycle perspective. In Section 2, the materials and methods are described. Section 3 presents the asymmetrical distribution of the HC anomalies during El Niño cycle, along with an exploration of the influence mechanism of SST anomalies on the HC variation. Finally, Section 4 comprises the discussion and conclusion.

2. Materials and Methods

We utilize the mass stream function (MSF) (Oort & Yienger, 1996) to capture the spatial structure of the HC based on four atmospheric reanalysis datasets from 1980 to 2018, namely, the Modern-Era Retrospective analysis for Research and Applications Version 2 (MERRA2) (Gelaro et al., 2017), National Centers for Environmental Prediction (NCEP)-Department of Energy Reanalysis 2 (NCEP2) (Kanamitsu et al., 2002), Japanese 55-year Reanalysis (JRA55) (Kobayashi et al., 2015), and European Centre for Medium-Range Weather Forecasts Era-Interim (ERAI) (Dee et al., 2011). Thirteen Atmospheric Model Intercomparison Project (AMIP) models (Table S1 in Supporting Information S1) from the Coupled Model Intercomparison Project6 (CMIP6) are used. The ensemble average over 13 models is derived by interpolating them into the same horizontal resolution of 2.5° × 2.5°. Three oceanic fields, including the National Oceanic and Atmospheric Administration (NOAA) Extended Reconstructed SST version 5 (ERSST5) (Huang et al., 2017), the Met Office Hadley Centre Sea Ice and SST data set (HadISST) (Rayner et al., 2003), and the Centennial in situ Observation-Based Estimates (COBE) SST version 1 (COBESST1) (Hirahara et al., 2014), are applied to estimate SST variations. According to the Climate Prediction Center, El Niño development and decay years are defined with a +0.5-threshold using the Niño 3.4 region's SST anomalies averaged over a three-month running period based on the Ocean Niño Index. If the criterion is satisfied for at least three consecutive seasons starting from autumn within a natural year, we consider that natural year as an El Niño development year (1982, 1986, 1991, 1994, 1997, 2002, 2004, 2006, 2009, and 2014). If there are three consecutive months with an anomaly index below 0.5 starting from summer within a natural year and the previous year was an El Niño year, we consider that natural year as an El Niño decay year (1983, 1988, 1992, 1995, 1998, 2003, 2005, 2007, 2010, and 2016). The selected years are consistent with those in previous studies (Li et al., 2020; Song et al., 2019; Wang & Zhang, 2002). It is worth mentioning that the events from 1986 to 1988 and 2014 to 2016 are treated as intense El Niño events (Allan et al., 2019; DiNezio et al., 2019). Therefore, 1986 and 2014 are categorized as development years, while 1988 and 2016 are classified as decay years. The MSF and SST in each calendar year are analyzed. When analyzing the modeled results,

19448007, 2023, 11, Downloaded from https://agupubs.onlinelibrary.wiley.com/doi/10.1029/2023GL103861 by Ocean University Of China, Wiley Online Library on [07/06/2023]. See the Terms and Conditions (https://onlinelibrary.wiley.com/terms-and-conditions) on Wiley Online Library for rules of use; OA articles are governed by the applicable Creative Commons License

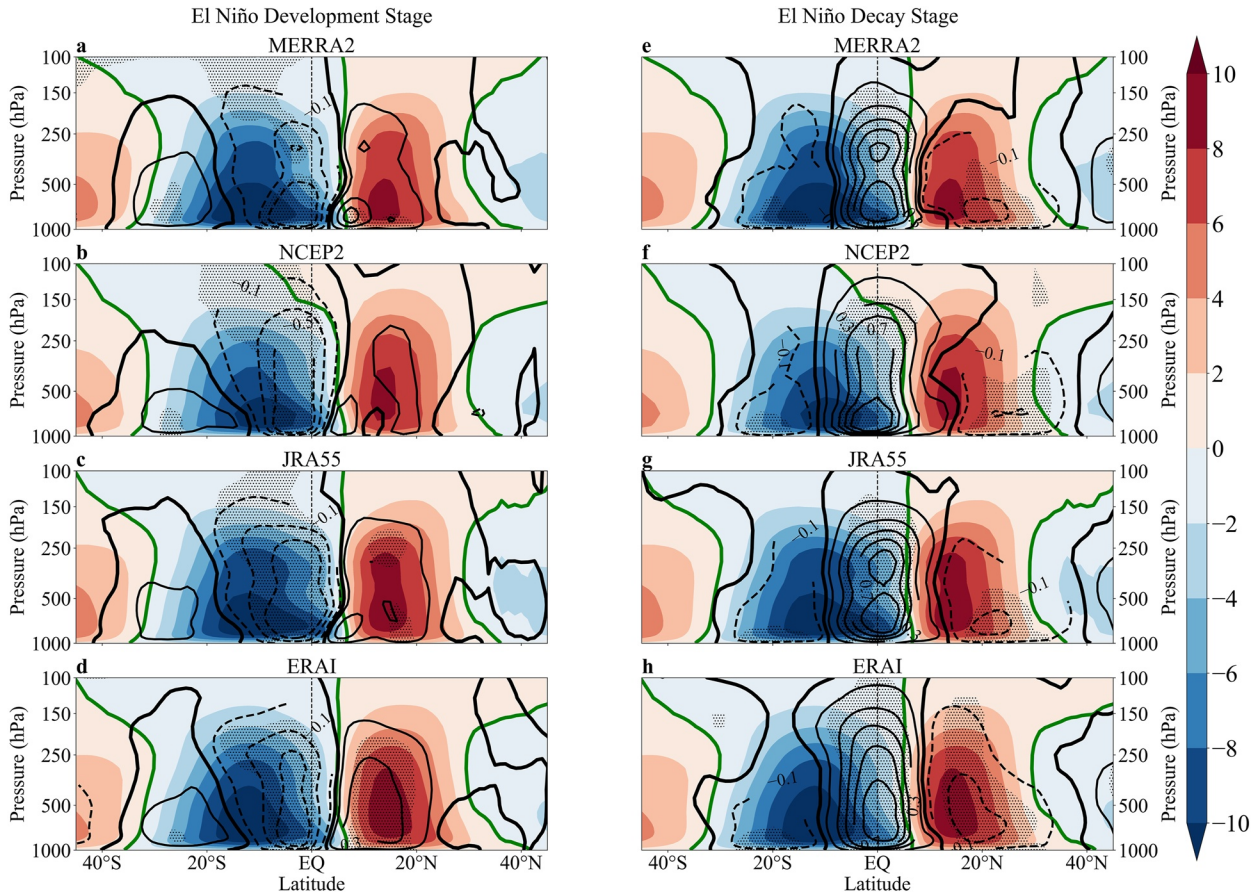

Figure 1. Spatial distribution of the climatological HC (shading, $\times 10^{10}$ kg s^{-1}) over the entire period and its anomalies (contour lines) during (left panel) El Niño development and (right panel) decay years based on (a), (e) MERRA2, (b), (f) NCEP2, (c), (g) MERRA2, and (d), (h) ERAI. The green line is the zero-value of climatic value. The solid (dotted) contour line is positive (negative), the contour interval is 0.2×10^{10} kg s^{-1}, and the zero line is thickened. The dark spot represents significance at the 0.05 level.

the years for the development and decay of El Niño do not include 2014 and 2016, respectively. The anomalies for MSF and SST were derived by calculating the composite value during development or decay stages and subtracting the climatic value from 1980 to 2018. A two-sided Student's *t*-test was employed to test the statistical significance.

3. Results

The spatial distribution of the climatological HC and its anomalous distribution during El Niño development and decay years are shown in Figure 1. The four datasets present a consistent spatial feature of the climatological HC (shadings in Figure 1), with an ascending branch at approximately 7°N and two descending branches at approximately 30° in the two hemispheres, presenting as an equatorial quasi-symmetric pattern. Additionally, the two Ferrell cells are observed north of 30°N and south of 30°S, indicating the transfer of angular momentum from the tropics to the polar regions (Hoskins & Yang, 2021). These findings highlight the importance of meridional flow and its impact on atmospheric circulation. In terms of the extent and intensity of the HC, the cells in the Southern Hemisphere (SH) perform more robustly than those in the Northern Hemisphere (NH), with an ~38° extent in the SH compared to an ~30° extent in the NH. Additionally, the equatorward location of the SH HC is much closer to the surface than that of the NH HC, indicating that there is deep penetration of the SH HC into the NH.

Moreover, the anomalous HC during El Niño development years (left panel of Figure 1), exhibits significant negative anomalies in the SH and opposite anomalies in the NH, displaying an equatorial symmetric pattern that aligns with the second mode of the HC anomaly discovered by Guo and Tan (2018b) and Sun and Zhou (2014).

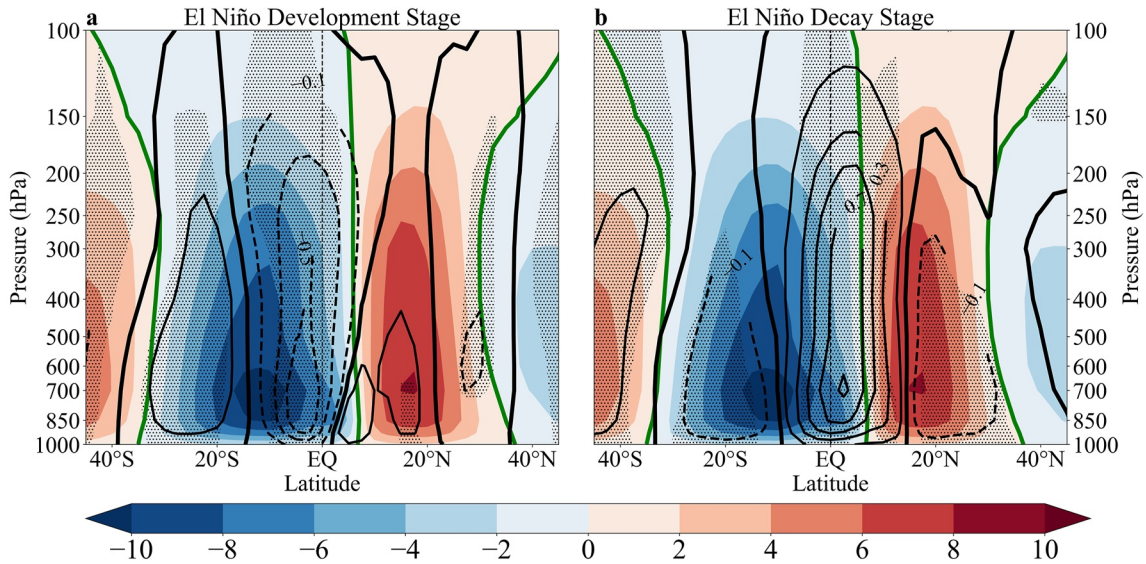

Figure 2. As in Figure 1, but for the climatological HC and its anomalies under the ensemble mean from 13 AMIP models.

Notably, the zero-value position of the HC anomaly near the equator basically coincides with that of the upward climatological HC. Moreover, two inverse anomaly distributions on either flank of the ascending motion of the climatological HC could strengthen the meridional circulation, consequently leading to greater transport of water vapor flux from the tropics to the subtropics.

However, the HC anomaly exhibits a different spatial pattern during El Niño decay years (right panel in Figure 1), presenting a prominent single cell with positive anomalies across the equator. This asymmetric mode ranges from 10°S to 10°N, which is consistent with the first mode of HC variability (Feng et al., 2019). The distribution indicates that positive values are strengthened from the upward branch of the climatological HC to the right subsiding branch of the HC anomaly, while negative values of the climatological HC in the area of positive anomalies are weakened. This suggests contrasting impacts on the Hadley cells of the NH and SH, where the NH cell is enhanced while the SH cell is diminished. Additionally, the different distribution of HC anomalies at different stages of El Niño have been manifested from other three indictors (velocity potential at 200 hPa, vertical shear of meridional wind (200–850 hPa) and vertical velocity, figures not shown). All the three indicators indicate that there is a significant upward movement with a southward shift and the vertical convection is strengthened during the decay stage. Consequently, this southward shift of the ascending motion would result in significantly less heat transport to the subtropics. The results show that El Niño has varying effects on the HC depending on its phase, leading to different conclusions in previous research.

Previous studies have shown that the HC varies depending on underlying thermal conditions, acting as a thermal-driving meridional circulation (Xie et al., 2022; Zaplotnik et al., 2022). The simulated climatological HC and the associated anomalies during El Niño development and decay years from 13 AMIP models (Figures S1 and S2 in Supporting Information S1) are consistent with those from reanalyses. This consistency is reflected in the strong correlation and standard deviation ratio, as depicted in Figures S3 and S4 in Supporting Information S1. Therefore, the 13 models support the hypothesis that anomalous SSTs during different stages of El Niño affect HC anomalies. Figure 2 shows the ensemble mean results during both stages. The ensemble averaged anomaly agrees well with the observed anomaly (red plus symbol from Figure S4 in Supporting Information S1), exhibiting spatial correlation coefficients of 0.88 and 0.90 during the development and decay stages, respectively. Although there is a subtle difference in the altitude position of the extremum, this difference does not affect overall consistency. Moreover, the simulations indicate noteworthy anomalies near the subtropical region (40°) in both hemispheres, which are absent in the reanalysis. This implies the occurrence of notable air–sea interactions (Emanuel et al., 1994; W Wu et al., 2011) in this region that cannot be captured by a simple ocean temperature-driven atmospheric circulation model.

Based on the reanalyses and simulations, it is evident that there is a notable contrast in the spatial distribution of HC anomalies between the development and decay years of El Niño. This disparity implies that the HC is

19448007, 2023, 11, Downloaded from https://agupubs.onlinelibrary.wiley.com/doi/10.1029/2023GL103861 by Ocean University Of China, Wiley Online Library on [07/06/2023]. See the Terms and Conditions (https://onlinelibrary.wiley.com/terms-and-conditions) on Wiley Online Library for rules of use; OA articles are governed by the applicable Creative Commons License

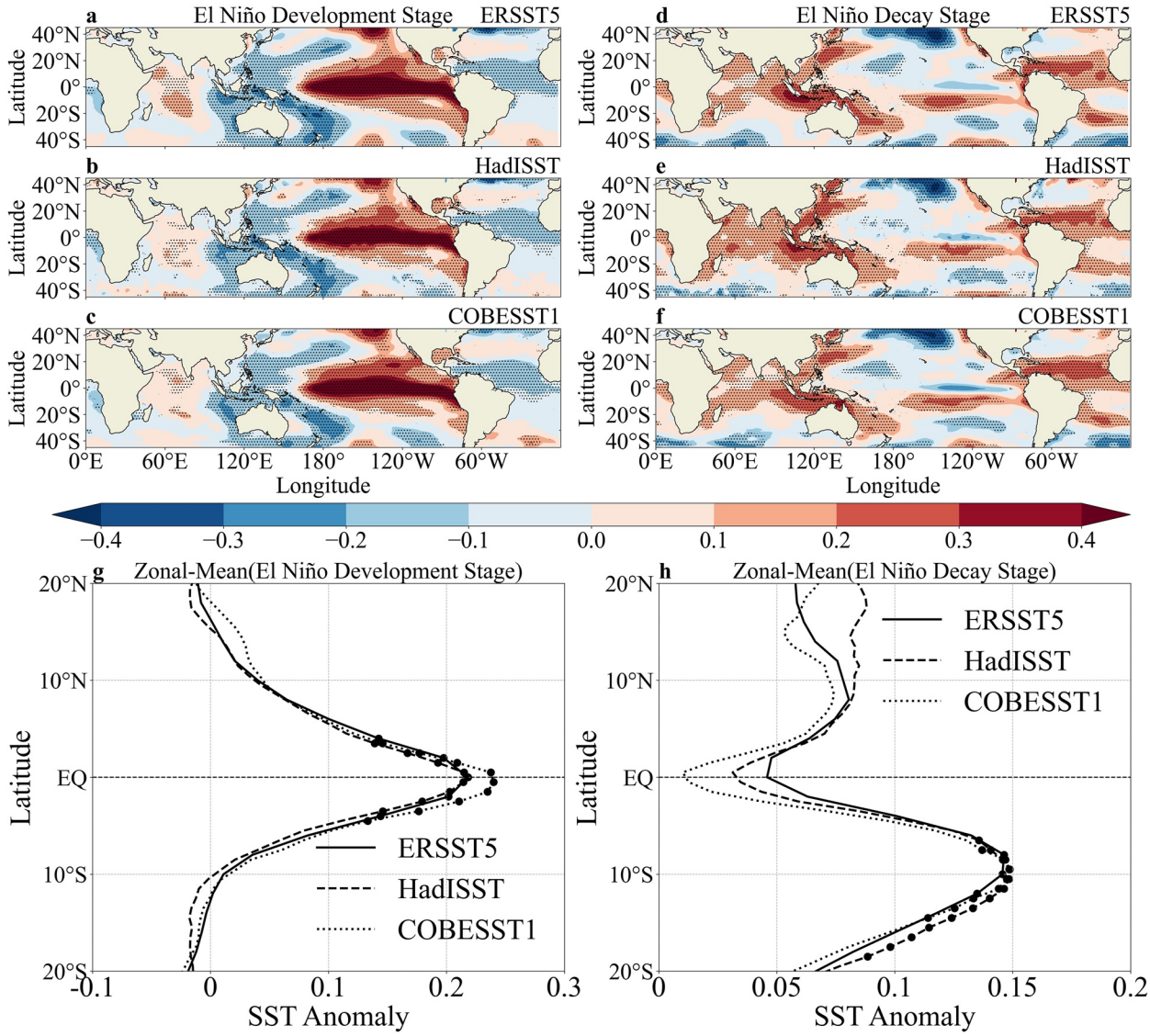

Figure 3. Composite SST anomalies during El Niño development (left panel) and decay years (right panel) based on the (a), (d) ERSST5, (b), (e) HadISST, and (c), (f) COBESST1 datasets. The dots in (a–f) represent significance at the 0.05 level. (g) The zonal-mean SST anomalies during El Niño development years. (h) Same as (g) but during El Niño decay years. The dark spots in (g and h) represent significance at the 0.1 level.

potentially influenced by distinct SST anomalies during each stage. Therefore, the spatial features of SST during the two stages are investigated.

Figure 3 depicts the spatial distribution of SST anomalies and their zonal-mean profiles during the development and decay stages. During development (Figures 3a–3c), significantly positive anomalies occur in the central and eastern Pacific Ocean, while evident negative anomalies are observed in the western Indo-Pacific Warm Pool, and slight negative anomalies appear in the tropical Atlantic Ocean. This distribution is attributed to the weakening of trade winds in the SH, which leads to a concurrent weakening of equatorial upwelling (Bjerknes, 1969). During decay, the SST anomalies exhibit a distinct spatial pattern (Figures 3d–3f). Notably, obvious positive anomalies appear in the tropical Indian Ocean and Atlantic Ocean, with the maximum in the southeastern Indo-Pacific Warm Pool, due to teleconnections between the ENSO and other tropical seas, as explained by Czaja et al. (2002), Kim et al. (2012) and R Wu et al. (2020). Additionally, opposite anomalies occur on the flanks of the equatorial central and eastern Pacific Ocean, with a positive feature south of the equator and a negative feature north of the equator, indicating an asymmetric decay rate of SST consistent with that reported in previous studies (McGregor et al., 2012; Song et al., 2022). This asymmetrical decay rate may be caused by the discordant zonal winds that

19448007, 2023, 11, Downloaded from https://agupubs.onlinelibrary.wiley.com/doi/10.1029/2023GL103861 by Ocean University Of China, Wiley Online Library on [07/06/2023]. See the Terms and Conditions (https://onlinelibrary.wiley.com/terms-and-conditions) on Wiley Online Library for rules of use; OA articles are governed by the applicable Creative Commons License

19448007, 2023, 11, Downloaded from https://agupubs.onlinelibrary.wiley.com/doi/10.1029/2023GL103861 by Ocean University Of China, Wiley Online Library on [07/06/2023]. See the Terms and Conditions (https://onlinelibrary.wiley.com/terms-and-conditions) on Wiley Online Library for rules of use; OA articles are governed by the applicable Creative Commons License

dominate the flanks of the equatorial Pacific Ocean. During decay, the zonal wind in the northern region of the equatorial Pacific Ocean is reigned by easterly winds, which induces equatorial ocean waves and causes thermocline changes, resulting in negative SST anomalies. Meanwhile, in the southern area of the equatorial Pacific Ocean, there is still a southward shift of the surface westerly, which was previously observed by Vecchi and Harrison (2006) and Sun and Zhou (2014). This shift causes shoaling of the eastern Pacific thermocline, resulting in a reduction in the overlying SST anomalies (Harrison & Vecchi, 1999). Consequently, the spatial features of SST anomalies exhibit dissimilarities across various stages of El Niño. The distinct SST anomalies observed during the two stages may correspond to differing SST meridional configurations that significantly influence the spatial distribution of the HC.

As shown in Figure 3g, the zonal-mean profile of SST anomalies during development displays an equatorial symmetric distribution with a maximum value of approximately 0.21°C near the equator. It has been reported that the SST field determines the location of low-level convergence (Schneider, 1977). Thus, the noteworthy equatorial symmetric SST anomalies would induce symmetrical anomalous meridional circulation, characterized by intensified upward movement in the vicinity of the equator. Meanwhile, an equatorial asymmetric SST profile is distributed during decay with the maximum at 10°S (Figure 3h). Oort and Rasmusson (1970) noted that even minor equatorial imbalances in the underlying surface temperature can markedly affect the spatial arrangement of the mean meridional circulation. This indicates that a shift of the thermal equator from the geodetic equator by several degrees of latitude can trigger asymmetrical equatorial circulation. Therefore, when the maximum positive anomaly shifts to 10°S, it may stimulate an equatorial asymmetric circulation anomaly (Figure 1). Essentially, we can assume that the meridional structures of SST anomalies linked with the development and decay stages might facilitate the emergence of the observed HC anomaly.

To further validate our assumption, we employ the Lindzen–Nigam model (Lindzen & Nigam, 1987) to provide theoretical verification. This model investigates the relationship between underlying thermal conditions and low-level atmospheric circulation in the tropics. The linearization formula is as follows:

$$-fV' = -\frac{g}{\alpha\cos\theta}\left[\left(2 - n\overline{T_s} + n\alpha H_0\right)\frac{\partial h'}{\partial\lambda} - \frac{nH_0}{2}\left(1 - \frac{2\gamma}{3}\right)\frac{\partial T_s'}{\partial\lambda}\right] - \epsilon U' \tag{1}$$

$$fU' = -\frac{g}{\alpha}\left[\left(2 - n\overline{T_s} + n\alpha H_0\right)\frac{\partial h'}{\partial\theta} - \frac{nH_0}{2}\left(1 - \frac{2\gamma}{3}\right)\frac{\partial T_s'}{\partial\theta} - \frac{\mathrm{nh}'}{2}\frac{\partial\overline{T_s}}{\partial\theta}\right] - \epsilon V' \tag{2}$$

where V' and U' are the derivatives of the meridional and zonal velocities with height, respectively. And f is the Coriolis parameter. g is gravity acceleration. α is the radius of the earth. n is the air expansion coefficient. H_0 denotes the boundary layer' height. T_s represents the SST, with an eddy component of T_s' and a mean state of $\overline{T}_s$. λ and θ are the longitude and latitude, respectively. h' is the horizontally inhomogeneous part, which is assumed to be much lower than H_0. γ is a constant. $\epsilon = Cd|V|_c/H_0$ is some constant typical wind speed in the trade cumulus boundary layer.

Through (1) × f-(2) × ϵ, we can obtain the following formula:

$$\begin{aligned}-f^2V' = &-\frac{g}{\alpha\cos\theta}\left[\left(2 - n\overline{T_s} + n\alpha H_0\right)\frac{\partial h'}{\partial\lambda} - \frac{nH_0}{2}\left(1 - \frac{2\gamma}{3}\right)\frac{\partial T_s'}{\partial\lambda}\right]\\ &+\frac{g}{\alpha}\left[\left(2 - n\overline{T_s} + n\alpha H_0\right)\frac{\partial h'}{\partial\theta} - \frac{nH_0}{2}\left(1 - \frac{2\gamma}{3}\right)\frac{\partial T_s'}{\partial\theta} - \frac{nh'}{2}\frac{\partial\overline{T_s}}{\partial\theta}\right] + \epsilon^2V'\end{aligned} \tag{3}$$

After averaging all the variables over the zonal region, the terms on the right-hand side of Equation 3 with respect to longitude become zero. Lindzen and Nigam (1987) noted that the values of h' and T_s' are very small, which allows us to assume that the gradient variation in the zonal direction is equal to 0. As a result, Equation 3 can be simplified as follows:

$$\|V'\| = \frac{1}{(f^2 + \epsilon^2)}\frac{ngh'}{2\alpha}\frac{\partial\|\overline{T_s}\|}{\partial\theta} \tag{4}$$

where f, ϵ, n, g, h', and α can be treated as constants that do not alter the positive or negative transformation of the equation. Therefore, the positive correlation between meridional wind and meridional gradient of zonal-mean

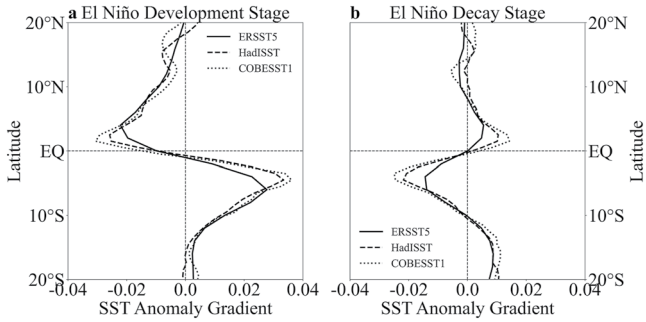

Figure 4. Meridional gradient distribution of zonal-mean SST anomalies with 3-point smoothing during El Niño (a) development and (b) decay years. Solid, dotted and dashed lines are based on ERSST5, HadISST, and COBESST1, respectively.

SST indicates that southerlies (northerlies) correspond to positive (negative) meridional SST gradients. Consequently, the zonal-mean SST meridional gradient's position shifts from a positive to a negative value, attains zero at the convergence location, and coincides with the ascending branch of the HC.

Consequently, the meridional gradient of the zonal-mean SST anomalies during the two stages of El Niño are examined. During development, the location where the meridional gradient equals zero is found to be around the equator (Figure 4a). In contrast, the location where the gradient is zero moves to approximately 10°S during decay (Figure 4b). This indicates that the reverse distribution of the HC anomaly is caused by the accompanying meridional gradient of SST, providing evidence that the different SST meridional gradients during the two stages determine the formation of the associated HC by regulating the location of the ascent.

4. Conclusion and Discussion

In this study, we investigate the effects of El Niño on the HC with a focus on its different stages. During development, an equatorial symmetric HC anomaly is observed, whereas during decay, an equatorial asymmetric HC anomaly with an anomalous ascent located at ∼10°S is observed. Meanwhile, the highly correlated simulation results from the AMIP models exhibit similar symmetric and asymmetric anomalous spatial structures, indicating that the variation in the HC anomaly is primarily associated with the thermal conditions of the underlying surface during distinct El Niño stages.

The SST datasets reveal that during development, the zonal-mean SST anomalies exhibit an equatorial symmetric structure, which stimulates an equatorially symmetric anomalous meridional circulation by adjusting the position of low-level convergence. However, during decay, the zonal-mean SST anomalies exhibit an asymmetric structure with a positive maximum located at 10°S corresponding with an anomalous ascent located to the south of the equator. This suggests that the distinct anomalous meridional circulation accompanied by different El Niño stages is mainly due to their parallel underlying SST meridional distribution. This point is further verified by theoretical deduction. Based on the theoretical model relating the underlying thermal force and low-level winds proposed by Lindzen and Nigam (1987), a simplified equation is derived, demonstrating that the meridional gradient of SST influence low-level convergence. This provides a theoretical explanation for why different HC anomalies are observed along with El Niño events, providing evidence that fluctuations in the meridional gradient of SST anomalies can stimulate the spatial distribution of meridional circulation. Therefore, our results explain the controversy regarding the impacts of El Niño on the HC anomaly. This is mainly because the associated SST anomalies during El Niño's development (decay) stages exhibit symmetric (asymmetric) structures resulting in symmetric (asymmetric) HC anomalies.

Importantly, there is a tripole mode over the subtropics of the North Pacific and a quadrupole mode over the South Pacific. These anomalous modes may also impact the HC, and analysis will be carried out in future work. Additionally, significant asymmetry in the decay rate between El Niño and La Niña events is highlighted (Hayashi et al., 2020; McGregor et al., 2012; Song et al., 2022). Following the mature phase of El Niño events, they usually progress into La Niña events in the following June-July period. According to studies by Okumura and Deser (2010) and Chen and Li (2021), the negative SST anomalies linked to La Niña events can last for over a year after peaking, they often regain strength in the subsequent winter season, which indicates that distinct spatial structures of SST anomalies exist during various stages of La Niña compared to El Niño. Therefore, it is worth further studying the impact of the different stages of La Niña on the HC. Additionally, SST exhibits different decay rates under different types of El Niño, which means SST exhibits different spatial anomalous signals over tropical region (Chen & Li, 2021). Once inconsistent anomalous signals occur, it will cause changes in the meridional structure of SST, and further trigger different HC anomalies. It is worth further studying the impact of distinct types of El Niño on the HC. Meanwhile, the anomalous HC at mid-latitudes has different signs depending on the phase of El Niño (Figure 1). This implies that the phase transition of El Niño can affect the poleward position of the HC, and it would be interesting to further detect the effects of El Niño's different stages on the HC boundary. Overall, our findings contribute to understanding why the impacts of the ENSO on the HC differed in previous studies and provide an explanation for the different effects. This result has significant

19448007, 2023, 11, Downloaded from https://agupubs.onlinelibrary.wiley.com/doi/10.1029/2023GL103861 by Ocean University Of China, Wiley Online Library on [07/06/2023]. See the Terms and Conditions (https://onlinelibrary.wiley.com/terms-and-conditions) on Wiley Online Library for rules of use; OA articles are governed by the applicable Creative Commons License

implications for future assessments and modeling of the climate impacts of ENSO and HC changes because both involve large-scale air–sea interactions.

Data Availability Statement

The atmospheric reanalyses including MERR2, NCEP2, JRA55, ERAI are available at https://disc.gsfc.nasa.gov/datasets?project=MERRA-2, https://psl.noaa.gov/data/gridded/data.ncep.reanalysis2.html, https://rda.ucar.edu/datasets/ds628.1/dataaccess/, and https://apps.ecmwf.int/datasets/data/interim-full-mnth/levtype=pl/, respectively. The oceanic reanalyses including ERSST5, HadISST and COBESST1 are available at https://psl.noaa.gov/data/gridded/data.noaa.ersst.v5.html, https://climatedataguide.ucar.edu/climate-data/sst-data-hadisst-v11, and https://psl.noaa.gov/data/gridded/data.cobe.html, respectively. The AMIP model's output from CMIP6 is available at https://esgf-node.llnl.gov/search/cmip6/.

Acknowledgments
This work was supported by the National Natural Science Foundation of China (42222501, 42130607, and 41975079), the Project of Southern Marine Science and Engineering Guangdong Laboratory (Zhuhai) under contract No. SML2020SP008.

References

Allan, R. J., Gergis, J., & D'Arrigo, R. D. (2019). Placing the AD 2014–2016 'protracted' El Niño episode into a long-term context. *The Holocene*, *30*(1), 90–105. https://doi.org/10.1177/0959683619875788

Bjerknes, J. (1969). Atmospheric teleconnections from the equatorial Pacific1. *Monthly Weather Review*, *97*(3), 163–172. https://doi.org/10.1175/1520-0493(1969)097<0163:atftep>2.3.co;2

Bordoni, S., & Schneider, T. (2010). Regime transitions of steady and time-dependent Hadley circulations: Comparison of axisymmetric and eddy-permitting simulations. *Journal of the Atmospheric Sciences*, *67*(5), 1643–1654. https://doi.org/10.1175/2009jas3294.1

Chen, M., & Li, T. (2021). ENSO evolution asymmetry: EP versus CP El Niño. *Climate Dynamics*, *56*(11–12), 3569–3579. https://doi.org/10.1007/s00382-021-05654-7

Czaja, A., van der Vaart, P., & Marshall, J. (2002). A diagnostic study of the role of remote forcing in tropical atlantic variability. *Journal of Climate*, *15*(22), 3280–3290. https://doi.org/10.1175/1520-0442(2002)015<3280:adsotr>2.0.co;2

Dee, D. P., Uppala, S. M., Simmons, A. J., Berrisford, P., Poli, P., Kobayashi, S., et al. (2011). The ERA-interim reanalysis: Configuration and performance of the data assimilation system. *Quarterly Journal of the Royal Meteorological Society*, *137*(656), 553–597. https://doi.org/10.1002/qj.828

DiNezio, P. N., Okumura, Y. M., & Wu, X. (2019). What controls the duration of El Niño and La Niña events? *Journal of Climate*, *32*(18), 5941–5965. https://doi.org/10.1175/jcli-d-18-0681.1

Emanuel, K. A., David Neelin, J., & Bretherton, C. S. (1994). On large-scale circulations in convecting atmospheres. *Quarterly Journal of the Royal Meteorological Society*, *120*(519), 1111–1143. https://doi.org/10.1002/qj.49712051902

Fang, M., & Tung, K. K. (1999). Time-dependent nonlinear Hadley circulation. *Journal of the Atmospheric Sciences*, *56*(12), 1797–1807. https://doi.org/10.1175/1520-0469(1999)056<1797:tdnhc>2.0.co;2

Feng, J., & Li, J. (2013). Contrasting impacts of two types of ENSO on the boreal spring Hadley circulation. *Journal of Climate*, *26*(13), 4773–4789. https://doi.org/10.1175/jcli-d-12-00298.1

Feng, J., Li, J., Jin, F., Liu, Z., Nan, X., & Guo, Y. (2016). Contrasting responses of the Hadley circulation to equatorially asymmetric and symmetric meridional sea surface temperature structures. *Journal of Climate*, *29*(24), 8949–8963. https://doi.org/10.1175/jcli-d-16-0171.1

Feng, J., Li, J., Jin, F.-F., Liu, Z., & Zhao, S. (2019). Effect of El Niño on the response ratio of Hadley circulation to different SST meridional structures. *Climate Dynamics*, *53*(7–8), 3877–3891. https://doi.org/10.1007/s00382-019-04756-7

Freitas, A. C. V., Aímola, L., Ambrizzi, T., & de Oliveira, C. P. (2016). Changes in intensity of the regional Hadley cell in Indian Ocean and its impacts on surrounding regions. *Meteorology and Atmospheric Physics*, *129*(3), 229–246. https://doi.org/10.1007/s00703-016-0477-6

Gelaro, R., McCarty, W., Suarez, M. J., Todling, R., Molod, A., Takacs, L., et al. (2017). The modern-era retrospective analysis for research and applications, version 2 (MERRA-2). *Journal of Climate*, *30*(13), 5419–5454. https://doi.org/10.1175/jcli-d-16-0758.1

Guo, Y.-P., & Tan, Z.-M. (2018a). On the sensitivity of the relationship between Hadley circulation asymmetry and ENSO in CMIP5 models. *Geophysical Research Letters*, *45*(17), 9253–9259. https://doi.org/10.1029/2018gl079515

Guo, Y.-P., & Tan, Z.-M. (2018b). Relationship between El Niño–Southern Oscillation and the symmetry of the Hadley circulation: Role of the sea surface temperature annual cycle. *Journal of Climate*, *31*(13), 5319–5332. https://doi.org/10.1175/jcli-d-17-0788.1

Hadley, G. (1735). VI. Concerning the cause of the general trade-winds. *Philosophical Transactions of the Royal Society of London*, *39*(437), 58–62.

Ham, Y. G., Lee, H. J., Jo, H. S., Lee, S., Cai, W., & Rodrigues, R. R. (2021). Inter-basin interaction between variability in the South Atlantic Ocean and the El Niño/Southern Oscillation. *Geophysical Research Letters*, *48*(15), e2021GL093338. https://doi.org/10.1029/2021gl093338

Harrison, D. E., & Vecchi, G. A. (1999). On the termination of El Niño. *Geophysical Research Letters*, *26*(11), 1593–1596. https://doi.org/10.1029/1999gl900316

Hayashi, M., Jin, F. F., & Stuecker, M. F. (2020). Dynamics for El Nino-La Nina asymmetry constrain equatorial-Pacific warming pattern. *Nature Communications*, *11*(1), 4230. https://doi.org/10.1038/s41467-020-17983-y

Hirahara, S., Ishii, M., & Fukuda, Y. (2014). Centennial-scale sea surface temperature analysis and its uncertainty. *Journal of Climate*, *27*(1), 57–75. https://doi.org/10.1175/jcli-d-12-00837.1

Hoskins, B. J., & Yang, G. Y. (2021). The detailed dynamics of the Hadley cell. Part II: December–February. *Journal of Climate*, *34*(2), 805–823. https://doi.org/10.1175/jcli-d-20-0504.1

Hoskins, B. J., Yang, G. Y., & Fonseca, R. M. (2020). The detailed dynamics of the June–August Hadley cell. *Quarterly Journal of the Royal Meteorological Society*, *146*(727), 557–575. https://doi.org/10.1002/qj.3702

Hu, Y., Huang, H., & Zhou, C. (2018). Widening and weakening of the Hadley circulation under global warming. *Science Bulletin*, *63*(10), 640–644. https://doi.org/10.1016/j.scib.2018.04.020

Huang, B., Thorne, P. W., Banzon, V. F., Boyer, T., Chepurin, G., Lawrimore, J. H., et al. (2017). Extended reconstructed sea surface temperature, version 5 (ERSSTv5): Upgrades, validations, and intercomparisons. *Journal of Climate*, *30*(20), 8179–8205. https://doi.org/10.1175/jcli-d-16-0836.1

19448007, 2023, 11, Downloaded from https://agupubs.onlinelibrary.wiley.com/doi/10.1029/2023GL103861 by Ocean University Of China, Wiley Online Library on [07/06/2023]. See the Terms and Conditions (https://onlinelibrary.wiley.com/terms-and-conditions) on Wiley Online Library for rules of use; OA articles are governed by the applicable Creative Commons License

Jiang, L., & Li, T. (2019). Relative roles of El Niño-induced extratropical and tropical forcing in generating Tropical North Atlantic (TNA) SST anomaly. *Climate Dynamics*, *53*(7–8), 3791–3804. https://doi.org/10.1007/s00382-019-04748-7

Kanamitsu, M., Ebisuzaki, W., Woollen, J., Yang, S. K., Hnilo, J. J., Fiorino, M., & Potter, G. L. (2002). NCEP–DOE AMIP-II reanalysis (R-2). *Bulletin of the American Meteorological Society*, *83*(11), 1631–1644. https://doi.org/10.1175/bams-83-11-1631(2002)083<1631:nar>2.3.co;2

Kim, S. T., Yu, J.-Y., & Lu, M.-M. (2012). The distinct behaviors of Pacific and Indian Ocean warm pool properties on seasonal and interannual time scales. *Journal of Geophysical Research*, *117*(D5), D05128. https://doi.org/10.1029/2011jd016557

Kobayashi, S., Ota, Y., Harada, Y., Ebita, A., Moriya, M., Onoda, H., et al. (2015). The JRA-55 reanalysis: General specifications and basic characteristics. *Journal of the Meteorological Society of Japan. Ser. II*, *93*(1), 5–48. https://doi.org/10.2151/jmsj.2015-001

Li, Y., Strapasson, A., & Rojas, O. (2020). Assessment of El Niño and La Niña impacts on China: Enhancing the early warning system on food and agriculture. *Weather and Climate Extremes*, *27*, 100208. https://doi.org/10.1016/j.wace.2019.100208

Lindzen, R. S., & Nigam, S. (1987). On the role of sea surface temperature gradients in forcing low-level winds and convergence in the tropics. *Journal of the Atmospheric Sciences*, *44*(17), 2418–2436. https://doi.org/10.1175/1520-0469(1987)044<2418:otross>2.0.co;2

Ma, J., & Li, J. (2008). The principal modes of variability of the boreal winter Hadley cell. *Geophysical Research Letters*, *35*(1), L01808. https://doi.org/10.1029/2007gl031883

McCreary, J. P., Xie, S. P., Annamalai, H., & Murtugudde, R. (2005). Impact of Indian Ocean sea surface temperature on developing El Niño. *Journal of Climate*, *18*(2), 302–319. https://doi.org/10.1175/jcli-3268.1

McGregor, S., Timmermann, A., Schneider, N., Stuecker, M. F., & England, M. H. (2012). The effect of the south Pacific convergence zone on the termination of El Nino events and the meridional asymmetry of ENSO. *Journal of Climate*, *25*(16), 5566–5586. https://doi.org/10.1175/jcli-d-11-00332.1

Nguyen, H., Evans, A., Lucas, C., Smith, I., & Timbal, B. (2013). The Hadley circulation in reanalyses: Climatology, variability, and change. *Journal of Climate*, *26*(10), 3357–3376. https://doi.org/10.1175/jcli-d-12-00224.1

Numaguti, A. (1995). Dynamics and energy balance of the Hadley circulation and the tropical precipitation zones. Part II: Sensitivity to meridional SST distribution. *Journal of the Atmospheric Sciences*, *52*(8), 1128–1141. https://doi.org/10.1175/1520-0469(1995)052<1128:daebot>2.0.co;2

Okumura, Y. M., & Deser, C. (2010). Asymmetry in the duration of El Niño and La Niña. *Journal of Climate*, *23*(21), 5826–5843. https://doi.org/10.1175/2010jcli3592.1

Oort, A. H., & Rasmusson, E. M. (1970). On the annual variation of the monthly mean meridional circulation. *Monthly Weather Review*, *98*(6), 423–442. https://doi.org/10.1175/1520-0493(1970)098<0423:otavot>2.3.co;2

Oort, A. H., & Yienger, J. J. (1996). Observed interannual variability in the Hadley circulation and its connection to ENSO. *Journal of Climate*, *9*(11), 2751–2767. https://doi.org/10.1175/1520-0442(1996)009<2751:oivith>2.0.co;2

Rayner, N. A., Parker, D. E., Horton, E. B., Folland, C. K., Alexander, L. V., Rowell, D. P., et al. (2003). Global analyses of sea surface temperature, sea ice, and night marine air temperature since the late nineteenth century. *Journal of Geophysical Research*, *108*(D14), 4407. https://doi.org/10.1029/2002jd002670

Schneider, E. K. (1977). Axially symmetric steady-state models of the basic state for instability and climate studies. Part II. Nonlinear calculations. *Journal of the Atmospheric Sciences*, *34*(2), 280–296. https://doi.org/10.1175/1520-0469(1977)034<0280:asssmo>2.0.co;2

Schott, F. A., Xie, S.-P., & McCreary, J. P. (2009). Indian Ocean circulation and climate variability. *Reviews of Geophysics*, *47*(1), RG1002. https://doi.org/10.1029/2007rg000245

Seager, R., Harnik, N., Kushnir, Y., Robinson, W., & Miller, J. (2003). Mechanisms of hemispherically symmetric climate variability. *Journal of Climate*, *16*(18), 2960–2978. https://doi.org/10.1175/1520-0442(2003)016<2960:mohscv>2.0.co;2

Song, X., Zhang, R., & Rong, X. (2019). Influence of intraseasonal oscillation on the asymmetric decays of El Niño and La Niña. *Advances in Atmospheric Sciences*, *36*(8), 779–792. https://doi.org/10.1007/s00376-019-9029-6

Song, X., Zhang, R., & Rong, X. (2022). Dynamic causes of ENSO decay and its asymmetry. *Journal of Climate*, *35*(2), 445–462. https://doi.org/10.1175/jcli-d-21-0138.1

Stuecker, M. F., Jin, F.-F., & Timmermann, A. (2015). El Niño–Southern Oscillation frequency cascade. *Proceedings of the National Academy of Sciences of the United States of America*, *112*(44), 13490–13495. https://doi.org/10.1073/pnas.1508622112

Sun, Y., & Zhou, T. (2014). How Does El Niño affect the interannual variability of the boreal summer Hadley circulation? *Journal of Climate*, *27*(7), 2622–2642. https://doi.org/10.1175/jcli-d-13-00277.1

Timmermann, A., An, S. I., Kug, J. S., Jin, F. F., Cai, W., Capotondi, A., et al. (2018). El Nino-Southern Oscillation complexity. *Nature*, *559*(7715), 535–545.

Vecchi, G. A., & Harrison, D. E. (2006). The termination of the 1997–98 El Niño. Part I: Mechanisms of oceanic change. *Journal of Climate*, *19*(12), 2633–2646. https://doi.org/10.1175/jcli3776.1

Wang, B., & Zhang, Q. (2002). Pacific–East Asian teleconnection. Part II: How the Philippine Sea anomalous anticyclone is established during El Niño development. *Journal of Climate*, *15*(22), 3252–3265. https://doi.org/10.1175/1520-0442(2002)015<3252:peatpi>2.0.co;2

Wu, R., Lin, M., & Sun, H. (2020). Impacts of different types of El Niño and La Niña on northern tropical Atlantic sea surface temperature. *Climate Dynamics*, *54*(9–10), 4147–4167. https://doi.org/10.1007/s00382-020-05220-7

Wu, W., Wen, Z., Wu, R., & Wang, T. (2011). Air–Sea interaction over the subtropical north Pacific during the ENSO transition phase. *Journal of Climate*, *24*(22), 5772–5785. https://doi.org/10.1175/2011jcli3820.1

Xie, X., Huang, P., Zhou, S., & Zhang, J. (2022). Changes in ENSO-driven Hadley circulation variability under global warming. *Atmospheric Research*, *274*, 106220. https://doi.org/10.1016/j.atmosres.2022.106220

Yu, M., Feng, J., Li, J., & An, R. (2022). Interdecadal shift of the El Niño's modulation on the connection between the Hadley circulation and tropical SST. *Climate Dynamics*, *60*(7–8), 2167–2181. https://doi.org/10.1007/s00382-022-06407-w

Zaplotnik, Ž., Pikovnik, M., & Boljka, L. (2022). Recent Hadley circulation strengthening: A trend or multidecadal variability? *Journal of Climate*, *35*(13), 4157–4176. https://doi.org/10.1175/jcli-d-21-0204.1

Zhang, G., & Wang, Z. (2013). Interannual variability of the Atlantic Hadley circulation in boreal summer and its impacts on tropical cyclone activity. *Journal of Climate*, *26*(21), 8529–8544. https://doi.org/10.1175/jcli-d-12-00802.1

19448007, 2023, 11, Downloaded from https://agupubs.onlinelibrary.wiley.com/doi/10.1029/2023GL103861 by Ocean University Of China, Wiley Online Library on [07/06/2023]. See the Terms and Conditions (https://onlinelibrary.wiley.com/terms-and-conditions) on Wiley Online Library for rules of use; OA articles are governed by the applicable Creative Commons License